Carbon nanotube-graphene junctions studied by impedance spectra

M. Gao, Z. L. Huang, B. Zeng, T. S. Pan, Y. Zhang, H. B. Peng, and Y. Lin

Citation: Applied Physics Letters **106**, 051601 (2015); doi: 10.1063/1.4907642
View online: http://dx.doi.org/10.1063/1.4907642
View Table of Contents: http://scitation.aip.org/content/aip/journal/apl/106/5?ver=pdfcov
Published by the AIP Publishing

Carbon nanotube-graphene junctions studied by impedance spectra

M. Gao,[1,a)] Z. L. Huang,[1] B. Zeng,[1] T. S. Pan,[1] Y. Zhang,[1] H. B. Peng,[2] and Y. Lin[1,3,a)]
[1]*State Key Laboratory of Electronic Thin Films and Integrated Devices, University of Electronic Science and Technology of China, Chengdu, Sichuan 610054, People's Republic of China*
[2]*Department of Physics and Texas Center for Superconductivity, University of Houston, Houston, Texas 77204-5005, USA*
[3]*Institute of Electronic and information Engineering in Dongguan, University of Electronic Science and Technology of China, Dongguan, Guangdong 523808, People's Republic of China*

(Received 13 November 2014; accepted 26 January 2015; published online 4 February 2015)

Two kinds of carbon nanotube (CNT)-graphene structures, vertical CNT-graphene and paralleled CNT–graphene, were fabricated to investigate the geometrical effect on the transport properties of the CNT–graphene junctions by using AC impedance spectra. The results demonstrated that the geometrical structure showed obvious impact on the resistance rather than the capacity of the junction. It is proposed that the difference caused by the geometrical structure may be associated with the dangling bonds terminated by –OH or –COOH of the open-ended CNTs. The unsymmetrical chemical bonds will increase the dipole moment in CNTs, which enhance the interaction between vertical CNTs and graphene and reduce the contact resistance. © *2015 AIP Publishing LLC*.
[http://dx.doi.org/10.1063/1.4907642]

The integrated structure of low dimensional carbon materials, such as graphene and carbon nanotube (CNT), is considered to be a potential candidate in applications such as interconnect, supercapacitors, and gas sensors due to its excellent electrical properties.[1–4] However, the junction between graphene and CNTs has great influence on the electrical properties of devices.[5] High resistance and capacity of the integrated structures would limit their applications in high frequency electrical devices. Thus, it is very important to systematically investigate the junction properties of CNT-graphene structures. Pei *et al*. fabricated a single CNT-graphene junction and found a Schottky barrier between the semiconducting CNT and graphene.[6] Cook *et al*. have calculated the transport properties of paralleled CNT-graphene contact.[7] And Novaes *et al*. investigated electron transport properties of covalently connected CNT-graphene via a first-principles study.[8] These studies have revealed that the junction properties may depend on the geometrical structure of graphene and CNT. However, systematic experimental investigations on the detailed impact of geometry on the electrical properties of CNT-graphene junctions are still lacking. The great challenges lie in the measurement and analysis of the electrical properties of the junction. On the other hand, impedance spectra have been widely used to investigate the transport properties of oxide films and nanotube networks.[9,10] Therefore, it would be valuable to explore the feasibility of studying the interfacial properties between CNTs and graphene by impedance spectra.

In this paper, to investigate the geometrical effect on the transport properties, we designed two types of CNT-graphene structures with aligned CNT arrays either parallel or vertical to the graphene plane. Then AC impedance measurement was used to check the conduction of junctions. We analyze the AC impedance spectra of both paralleled CNT-graphene and vertical CNT-graphene junctions to study the interfacial properties between graphene and CNT.

Aligned CNT arrays were prepared by using a floating chemical vapor deposition (CVD) method, as reported in literatures.[11,12] Methylbenzene (C_7H_8) was used as the liquid carbon sources and mixed with ferrocene (2 wt. %) to prepare the precursor. A floating catalyst CVD was employed in a two-stage furnace equipped with a horizontal quartz tube to synthesize CNTs on silicon substrates. The temperatures at preheating stage and decomposition stage were maintained at 250 °C and 800 °C, respectively. The precursor was introduced into the reactor with a rate of 6 ml/h in a carrier gas, which is a mixture of Ar (600 standard-state cubic centimeter per minute (sccm)) and H_2 (30 sccm). After 30 min growth, the height of the aligned CNT arrays can reach 2 mm. Then, CNT arrays can be detached from the silicon substrates and form solid aligned CNT cuboids. The photograph and SEM image of a vertical aligned CNT sample is showed in Figs. 1(a) and 1(b). The length and width of the CNT cuboid was about 10 mm and 2 mm, respectively. Meanwhile, graphene films were grown on copper foils by the CVD technique and

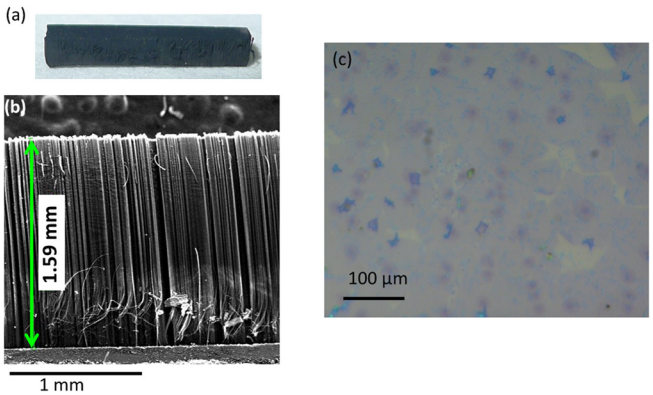

FIG. 1. (a) The photograph of CNTs. (b) SEM image of CNTs. (c) The photograph of the transferred graphene films on a SiO_2 substrate.

[a)]Authors to whom correspondence should be addressed. Electronic addresses: mingao@uestc.edu.cn and linyuan@uestc.edu.cn.

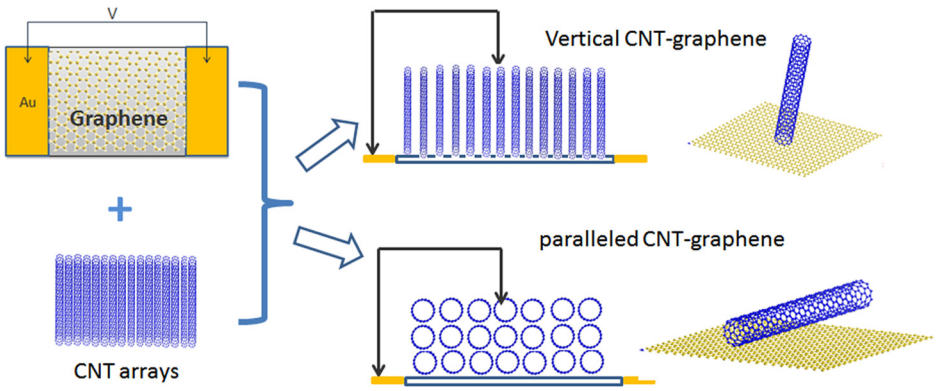

FIG. 2. The schematic drawing of two kinds of CNT/graphene structure.

then transferred on silicon dioxide substrates using polymethyl methacrylate (PMMA), as reported in literatures.[13–15] The photograph of the transferred graphene films on a SiO_2 substrate is shown in Fig. 1(c). The color contrast presents the thickness variation of the graphene films.

We designed two kinds of structures to investigate the contact properties of graphene and CNTs. The schematic drawing is shown in Fig. 2. Gold electrodes were prepared to electrically contact the graphene films from the bottom. After that CNT arrays were put on to the graphene films to form two kinds of CNT-graphene structures: vertical CNT-graphene and paralleled CNT-graphene. Agilent 4294A was used to measure the impedance spectra of the graphene, CNTs, and the CNT-graphene structures, respectively. Specifically, the measurement setup for the CNT-graphene structures is shown in Fig. 2, i.e., one probe contacted with the CNT arrays directly and the other probe contacted with the gold electrode on the graphene film. Owing to the good alignment of CNT arrays, difference in the spectra of these two kinds of CNT-graphene structures can be detected and used to analyze the junction properties.

To minimize the impact from electrodes on the AC impedance results, the contacts between the as-prepared samples and gold electrodes were examined by electrical transport measurements. The linear I-V curves of the as-prepared graphene films (not shown here) confirmed Ohmic contacts between the graphene and the gold electrodes.

For the measurement of impedance spectra in these samples, the frequency was changed from 50 Hz to 10 MHz and the signal amplitude was 500 mV. All experiments were conducted at room temperature. We should note that for graphene and CNTs, the impedance spectrum is independent on the applied bias voltage. The impedance spectra with zero bias voltage for CNTs, graphene, vertical CNT-grapheme, and paralleled CNT-graphene are shown in Figs. 3(a)–3(d), respectively. The results show that the CNT sample in this study exhibits a behavior like a pure resistance when the frequency is below 1 MHz and like an inductance at a higher frequency, as shown in Fig. 3(a). The as-prepared graphene and CNT-graphene samples all exhibit combinative behaviors of the resistance and capacity, varying with the frequency. This is reasonable considering the quality of the as-prepared graphene. The as-prepared graphene samples have several layers as indicated by the color of the transferred graphene layers on the silicon dioxide substrate. In addition, the as-prepared graphene samples also have many domains in large scale, as demonstrated by the color variation shown in Fig. 1(c). The resistance and capacity between the individual

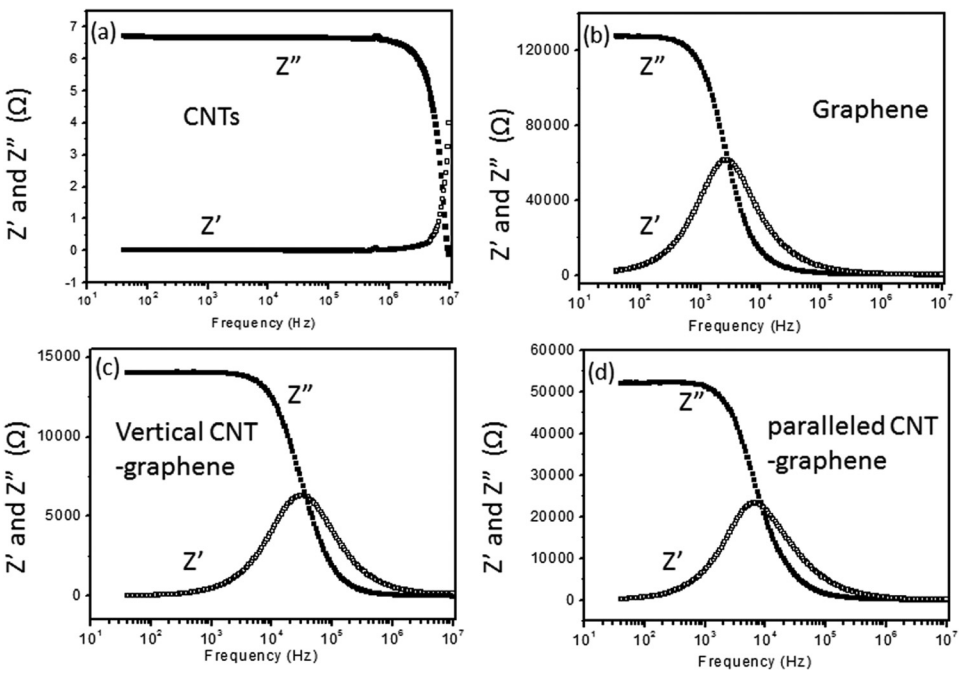

FIG. 3. The impedance spectra of CNTs (a), graphene (b), vertical CNT-graphene (c), and paralleled CNT-graphene (d).

layers and induced by the domain boundaries would both contribute to the impedance spectra of the as-prepared samples with the graphene films. Moreover, it is interesting to notice that the falloff frequency, i.e., the point where the sharp drop occurs in the real impedance, is shifted to higher frequency for the CNT-graphene samples in Figures 3(c) and 3(d) than that for the graphene sample in Figure 3(b).

To analyze the impedance spectra, the Nyquist plots for the as-prepared graphene, vertical CNT-graphene, and paralleled CNT-graphene samples are shown in Fig. 4. Although the spectra are all shaped in asymmetrical 1/2 semicircle, we use a simple equivalent circuit to analyze it. In CNT system, the equivalent circuit 1 in Fig. 4 was applied to fit the impedance spectra. But in our results, we found that the value of R_0 is far less than that of R, which means the resistance between junctions or domains dominate the transport properties in CNTs and graphene films. To simplify the analysis, we tried to use a simple parallel RC circuit (equivalent circuit 2 in Fig. 4) to fit the data and estimate the difference between the interfacial properties of these two kinds of geometric configuration.

For a simple parallel RC circuit, the frequency of the maximum imaginary impedance can be expressed as the following:[16]

$$f = \frac{1}{2\pi RC}, \tag{1}$$

where R is the resistance and C is the capacity of the sample. The resistance of CNT-graphene sample is equaled to real impedance at low frequency. By using Eq. (1) and the data extracted from Fig. 3, the frequency at the maximum imaginary impedance, the resistance, the calculated capacity, and the calculated ratio of resistance to capacity for three kinds of samples (the graphene, the vertical CNT-graphene, and the paralleled CNT -graphene) are listed in Table I. The ratio of resistance to capacitive will be used to present the contact properties of the sample, which is a common method to analyze the impedance spectra. Because the resistance of CNT arrays is very low (7 Ω as shown in Fig. 3(a)), the main contribution to the resistance of CNT-graphene samples comes from the graphene films and the junctions between the graphene and CNTs. It is obvious that the value of RC is the largest for graphene in Table I. As we know, single crystal graphene layer generally has low resistance.[17] Thus, the experimental result implies that the electrical transport properties of our graphene sample are determined mainly by the

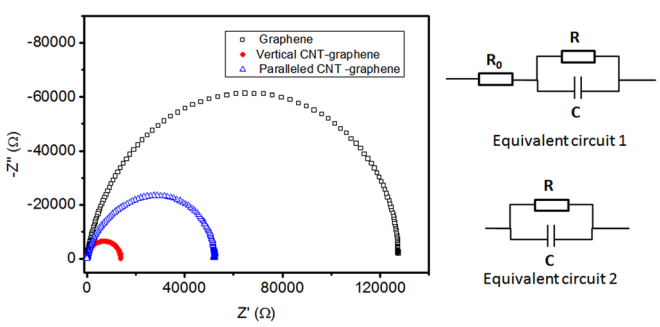

FIG. 4. The Nyquist plots for graphene, vertical CNT-graphene, and paralleled CNT-graphene.

TABLE I. The frequency at the maximum imaginary impedance, resistance, calculated capacity, and the calculated ratio of resistance to capacitive for graphene, vertical CNT-graphene, and paralleled CNT-graphene from Fig. 3.

Sample	Frequency (Hz)	Resistance (kΩ)	Capacity (pF)	R/C (kΩ/pF)
Graphene	2734	127.5	457	0.28
Vertical CNT-graphene	30899	14.0	368	0.04
Paralleled CNT -graphene	6534	51.9	469	0.11

resistive and capacitive contribution of the domain boundaries between graphene flakes.

Comparing the two kinds of graphene-CNT structures, we can see that the paralleled CNT-graphene junction has a 4-times-higher contact resistance than the vertical one. But the capacitive values for graphene and two kinds of CNT-graphene structures are at the same order of magnitude. The difference in the resistance of the two kinds of CNT-graphene structures is likely to come from the different interaction of the CNT-graphene junction. Graphene films and CNTs interact through van der Waals force, which is caused by the dispersion of dipole operators.[18] It is well known that CNTs may be open-ended or close-ended. Generally, the open-ended CNTs have better electrical contact with the substrates.[19] Although CNTs prepared by the floating CVD method are mostly closed-ended, it is possible that some of the CNTs are open-ended due to the etching of hydrogen atoms during the growing process. Moreover, the contact properties of the samples can be better reflected by the ratio of resistance to capacity. As seen in Table I, it is also indicated that the ratio of resistance to capacity for the vertical CNT-graphene is smaller than that for the paralleled CNT-graphene, which suggested that the interfacial properties between graphene and CNT are related to the geometrical structure. In our results, the impedance spectra show that resistance between junctions or domains dominate the transport properties in CNTs and graphene films. That is why we can ignore the resistance of CNTs, and we think that the difference ratio of resistance to capacity comes from the contact between graphene and carbon nanotubes. As mentioned above, the CNTs can be open or closed tubes.[20] For open-ended CNTs, carbon atoms at the end of the tubes have dangling bonds, which are not stable and can be easily terminated by –OH or –COOH in ambient conditions.[21] Then the X-ray Photoelectron Spectroscopy (XPS) of the carbon nanotubes was checked to confirm the properties of carbon atoms. In the supplementary material, Figure 1s is the XPS spectra of the carbon nanotubes.[22] Besides the main peak of C1s located at 284.6 eV, it had other three peaks, located at 286.5 eV, 288.3 eV, and 291 eV, respectively. According to previous studies,[23–25] the 286.5 eV and 288.3 eV peaks associated with –C–OH, –C=O and –COOH groups and the 291 eV peak associated with π-π*shake up. Our XPS results confirmed carbon atoms in our experiments bonded with other atoms. We know that CNT and graphene are nonpolar crystal. But when carbon dangling bonds are terminated by other atoms, the unsymmetrical chemical bonds will increase the dipole moment in CNTs. Then, the van der Waals force

can also be enhanced, which decrease the contact resistance between vertical CNTs and graphene. Thus, enhanced electrical contacting properties can be achieved in the vertical CNT-graphene structure comparing to the paralleled CNT-graphene. It should also be noted that the ratio of resistance to capacity for graphene is the highest in Table I. As the discussion above, we suggest that the resistance and capacity for graphene come from the domain boundaries. The results indicated that the contact resistance between domains of graphene flakes dominates the electric behavior rather than the capacity, which may originate from the discontinuity of the transferred graphene with large scale. The longer path on the graphene sheet between the two electrodes for the graphene sample than the CNT-graphene samples contains more domain boundaries, thus leading to a higher ratio of resistance to capacity for the graphene sample.

Meanwhile, the capacity for different junctions is of the same order of magnitude. This is reasonable since the capacity is determined by the distance and area of the electrode. For different geometrical structure of graphene and CNTs junction, the distance and junction area between graphene and CNTs may be almost the same. This is because that graphene films and CNTs interact through van der Waals force, so the different equilibrium distance for different atoms or molecules was neglected compared to the distance between graphene and carbon nanotubes. Thus, decreasing the distance between electrodes is a feasible way to decrease the capacity, which will be benefit for high frequency electrical devices. This result implies that the geometrical structure of graphene and CNTs junction itself has little influence on the capacity. However, to investigate and confirm the phenomena, further calculation is needed.

In summary, we developed two kinds of graphene-CNT structures and used their impedance spectra to analyze the junction properties between the graphene and CNTs. The result shows that the resistance of the junction depends on the geometrical structure of the junction, and meanwhile, the capacity of the junction is almost at the same order of magnitude. We think that the phenomena may be associated with the dipole moment of carbon atoms at the open ended CNTs. Our results demonstrate that impedance spectra analysis is a powerful method to study the contacting properties between graphene and CNTs, which may be helpful to enhance the performance of CNT-graphene based devices.

This work was supported by the National Basic Research Program of China (973 Program) under Grant No. 2015CB351905, the National Natural Science Foundation of China (No. 61306015), and Guangdong Innovative Research Team Program (No. 201001D0104713329).

[1]V. Jousseaume, J. Cuzzocrea, N. Bernier, and V. T. Renard, Appl. Phys. Lett. **98**(12), 123103 (2011).
[2]D. Yu and L. Dai, J. Phys. Chem. Lett. **1**(2), 467 (2010).
[3]Z. Fan, J. Yan, L. Zhi, Q. Zhang, T. Wei, J. Feng, M. Zhang, W. Qian, and F. Wei, Adv. Mater. **22**(33), 3723 (2010).
[4]H. Y. Jeong, D.-S. Lee, H. K. Choi, D. H. Lee, J.-E. Kim, J. Y. Lee, W. J. Lee, S. O. Kim, and S.-Y. Choi, Appl. Phys. Lett. **96**(21), 213105 (2010).
[5]Y. L. Kim, H. Y. Jung, S. Kar, and Y. J. Jung, Carbon **49**(7), 2450 (2011).
[6]T. Pei, H. T. Xu, Z. Y. Zhang, Z. X. Wang, Y. Liu, Y. Li, S. Wang, and L. M. Peng, Appl. Phys. Lett. **99**(11), 113102 (2011).
[7]B. G. Cook, W. R. French, and K. Varga, Appl. Phys. Lett. **101**(15), 153501 (2012).
[8]F. D. Novaes, R. Rurali, and P. Ordejon, ACS Nano **4**(12), 7596 (2010).
[9]M. P. Garrett, I. N. Ivanov, R. A. Gerhardt, A. A. Puretzky, and D. B. Geohegan, Appl. Phys. Lett. **97**(16), 163105 (2010).
[10]A. Tschope, E. Sommer, and R. Birringer, Solid State Ionics **139**(3–4), 255 (2001).
[11]B. Q. Wei, R. Vajtai, Y. Jung, J. Ward, R. Zhang, G. Ramanath, and P. M. Ajayan, Nature **416**(6880), 495 (2002).
[12]X. Li, A. Cao, Y. J. Jung, R. Vajtai, and P. M. Ajayan, Nano Lett. **5**(10), 1997 (2005).
[13]X. Li, W. Cai, J. An, S. Kim, J. Nah, D. Yang, R. Piner, A. Velamakanni, I. Jung, E. Tutuc, S. K. Banerjee, L. Colombo, and R. S. Ruoff, Science **324**(5932), 1312 (2009).
[14]C. Mattevi, H. Kim, and M. Chhowalla, J. Mater. Chem. **21**(10), 3324 (2011).
[15]C. Diaz-Pinto, D. De, V. G. Hadjiev, and H. Peng, ACS Nano **6**(2), 1142 (2012).
[16]L. C. Zou and C. Hunt, J. Electrochem. Soc. **156**(1), C8 (2009).
[17]K. S. Kim, Y. Zhao, H. Jang, S. Y. Lee, J. M. Kim, J. H. Ahn, P. Kim, J. Y. Choi, and B. H. Hong, Nature **457**(7230), 706 (2009).
[18]M. Bordag, B. Geyer, G. L. Klimchitskaya, and V. M. Mostepanenko, Phys. Rev. B **74**(20), 205431 (2006).
[19]L. B. Zhu, Y. Y. Sun, D. W. Hess, and C. P. Wong, Nano Lett. **6**(2), 243 (2006).
[20]X. Yang, L. Yuan, V. K. Peterson, Y. Yin, A. I. Minett, and A. T. Harris, J. Phys. Chem. C **115**(29), 14093 (2011).
[21]Z. Liu, K. Suenaga, P. J. F. Harris, and S. Iijima, Phys. Rev. Lett. **102**(1), 015501 (2009).
[22]See supplementary material at http://dx.doi.org/10.1063/1.4907642 for the XPS spectra of carbon nanotubes.
[23]A. F. Lee, Z. Chang, P. Ellis, S. F. J. Hackett, and K. Wilson, J. Phys. Chem. C **111**(51), 18844 (2007).
[24]A. F. Lee, J. N. Naughton, Z. Liu, and K. Wilson, ACS Catal. **2**(11), 2235 (2012).
[25]I. Kvande, J. Zhu, T. J. Zhao, N. Hammer, M. Ronning, S. Raaen, J. C. Walmsley, and D. Chen, J. Phys. Chem. C **114**(4), 1752 (2010).